https://doi.org/10.1093/plcell/koab286 THE PLANT CELL 2022: 34: 818–833

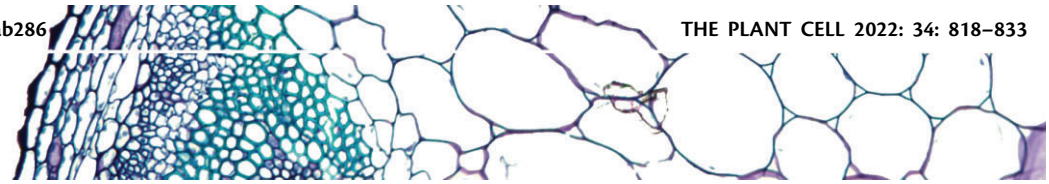

Research Article

A Molecular switch for *FLOWERING LOCUS C* activation determines flowering time in Arabidopsis

Lisha Shen [1,*,†] **Yu Zhang**[1,2] **and Nunchanoke Sawettalake** [1]

1 Temasek Life Sciences Laboratory, 1 Research Link, National University of Singapore, Singapore 117604, Singapore
2 Department of Biological Sciences, National University of Singapore, Singapore 117543, Singapore

*Author for correspondence: lisha@tll.org.sg
These authors contributed equally (L.S. and Y.Z.).
†Senior author.

L.S. conceived and designed the study. L.S., Y.Z., and N.N. performed the experiments. L.S. and Y.Z. analyzed data. L.S. wrote the paper. All authors read and approved the article.
The author responsible for distribution of materials integral to the findings presented in this article in accordance with the policy described in the instructions for Authors (https://academic.oup.com/plcell) is: Lisha Shen (lisha@tll.org.sg).

Abstract

Plants have evolved sophisticated mechanisms to ensure flowering in favorable conditions for reproductive success. In the model plant *Arabidopsis thaliana*, FLOWERING LOCUS C (FLC) acts as a central repressor of flowering and the major determinant for winter cold requirement for flowering. *FLC* is activated in winter annuals by the FRIGIDA (FRI) activator complex containing FRI, FLC EXPRESSOR (FLX), and FLX-LIKE 4 (FLX4), among which FLX and FLX4 are also essential for establishing basal *FLC* expression in summer annuals. Here we show that a plant RNA polymerase II C-terminal domain phosphatase, C-TERMINAL DOMAIN PHOSPHATASE-LIKE 3 (CPL3), interacts with and dephosphorylates FLX4 through their scaffold protein FLX to inhibit flowering. CPL3-mediated dephosphorylation of FLX4 serves as a key molecular switch that enables binding of dephosphorylated FLX4 to the *FLC* locus to promote *FLC* expression, thus repressing flowering in both winter and summer annuals of Arabidopsis. Our findings reveal a molecular switch underlying the activation of *FLC* for flowering time control.

Introduction

Flowering at the appropriate time is fundamental to the sexual reproductive success of higher plants. In the model plant *Arabidopsis thaliana*, this flowering process is tightly regulated by a complex network of genetic pathways, including photoperiod, vernalization, thermosensory, autonomous, gibberellin, and age pathways to ensure the timely initiation of flowering (Andres and Coupland, 2012; Pose et al., 2012; Bao et al., 2020). *FLOWERING LOCUS C* (*FLC*), encoding a MADS-box domain protein, acts as a central repressor of flowering through directly suppressing the transcription of two floral pathway integrators, *FLOWERING LOCUS T* (*FT*) and *SUPPRESSOR OF OVEREXPRESSION OF CONSTANS 1* (*SOC1*; Michaels and Amasino, 1999; Sheldon et al., 2000; Hepworth et al., 2002; Helliwell et al., 2006; Searle et al., 2006; Li et al., 2008; Whittaker and Dean, 2017).

Regulation of *FLC* expression is closely relevant to the natural variation in flowering time of different Arabidopsis accessions. Arabidopsis accessions can be categorized into two groups: winter annuals and summer annuals, based on their requirement for vernalization (a long period of winter cold) for rapid flowering. Summer annuals, also known as rapid-cycling accessions, flower quickly without vernalization. In contrast, winter annuals are very late flowering without vernalization, conferred by functional alleles of both

Received September 21, 2021. Accepted November 11, 2021. Advance access publication November 19, 2021

FRIGIDA (*FRI*) and *FLC* (Clarke and Dean, 1994; Koornneef et al., 1994; Lee et al., 1994a; Michaels and Amasino, 1999; Johanson et al., 2000). In winter annuals, FRI elevates *FLC* expression to levels that inhibit flowering (Johanson et al., 2000).

Genetic screening and molecular studies have identified many genes required for the activation of *FLC* by FRI. These genes could be tentatively divided into two groups, *FLC*-specific regulators and *FLC*-nonspecific regulators, based on whether they have other phenotypes in addition to flowering defects (Choi et al., 2011; Ding et al., 2013). *FLC*-nonspecific regulators, whose mutants have pleiotropic phenotypes, are mostly shown or predicted to possess chromatin-associated functions (Zhang and van Nocker, 2002; He et al., 2004; Oh et al., 2004; Jiang et al., 2009; Xu et al., 2009; Park et al., 2010; Yu and Michaels, 2010; Kim and Sung, 2012), whereas *FLC*-specific regulators, whose mutants mainly show flowering defects, include FRI-LIKE 1 (FRL1), FRL2, FRI-ESSENTIAL 1 (FES1), SUPPRESSOR OF FRI 4 (SUF4), FLC EXPRESSOR (FLX), and FLX-LIKE 4 (FLX4; also known as FLL4; Michaels et al., 2004; Schmitz et al., 2005; Kim et al., 2006; Kim and Michaels, 2006; Andersson et al., 2008; Choi et al., 2011; Ding et al., 2013; Lee and Amasino, 2013).

FRI functions as a scaffold protein to interact with these *FLC*-specific regulators, including FRL1, FES1, SUF4, FLX, and FLX4, to form the FRI-C transcription activator complex (Choi et al., 2011; Ding et al., 2013). Intriguingly, FRI-C is associated with multiple histone modifiers, including HISTONE ACETYLTRANSFERASE OF THE MYST FAMILY 1, the histone methyltransferase COMPASS-like complex, and the H2B ubiquitination ligase UBIQUITIN-CONJUGATING ENZYME 1, to form the FRI supercomplex that creates an active chromatin state at *FLC* for establishing the winter-annual growth habit (Li et al., 2018). Vernalization represses FRI-mediated *FLC* upregulation in response to a prolonged cold exposure, resulting in accelerated flowering (Sheldon et al., 2000; Michaels and Amasino, 2001).

In contrast to the winter annuals, the rapid-cycling accessions have a nonfunctional *fri* allele or a weak *flc* allele or both (Johanson et al., 2000; Gazzani et al., 2003; Michaels et al., 2003). Genetic screening of the rapid-cycling accessions has uncovered a group of genes that repress *FLC* in the autonomous pathway, including *FCA*, *FPA*, *FVE*, *LUMINIDEPENDENS*, *FLOWERING LOCUS D* (*FLD*), *FY*, and *FLOWERING LOCUS K* (*FLK*; Lee et al., 1994b; Macknight et al., 1997; Schomburg et al., 2001; He et al., 2003; Simpson et al., 2003; Ausin et al., 2004; Mockler et al., 2004). In addition, in the Columbia (Col) background, which contains a naturally occurring null allele of *fri*, several *FLC*-specific regulators, *FES1*, *SUF4*, *FLX*, and *FLX4*, but not *FRL1*, are required for the basal levels of *FLC* expression in the absence of *FRI* (Ding et al., 2013).

Here, we report that *FLC* activation is regulated by an RNA polymerase II (Pol II) C-terminal domain (CTD) phosphatase-like protein, C-TERMINAL DOMAIN PHOSPHATASE-LIKE 3 (CPL3). CPL3 is a member of the Arabidopsis Pol II CTD phosphatase family, which is categorized into three groups (Jin et al., 2011). CPL3 contains a catalytic domain similar to that of Fcp1 phosphatases in yeast and human and a BRCA1 C Terminus (BRCT) domain (Koiwa et al., 2002). Fcp1 dephosphorylates the serine-rich CTD of the largest subunit of Pol II to promote mRNA processing (Cho et al., 1999, 2001). Similarly, CPL3 has been shown to mediate the dephosphorylation of Pol II to regulate plant immune responses (Koiwa et al., 2004; Li et al., 2014). In this study, we show that CPL3-mediated dephosphorylation of FLX4 serves as a key molecular switch for promoting *FLC* expression in both winter and summer Arabidopsis accessions to inhibit flowering. CPL3 interacts with and dephosphorylates FLX4 via their common interacting protein FLX. CPL3-mediated dephosphorylation of FLX4 facilitates the binding of FLX4 to the *FLC* locus to promote *FLC* expression, thus repressing flowering. Overall, our study uncovers a molecular switch required for *FLC* activation, which is indispensable for controlling flowering time in Arabidopsis.

Results

CPL3 represses flowering in Arabidopsis

To study the biological function of *CPL3* during plant development, we identified three T-DNA insertion mutants, *cpl3–7*, *cpl3–8*, and *cpl3–9*, in the Col background from the Arabidopsis Information Resource (Figure 1A). There were no detectable *CPL3* transcripts spanning the T-DNA insertion sites in these homozygous mutant lines (Figure 1B). Partial *CPL3* transcripts upstream of the T-DNA insertion sites were detected in these mutants, while *CPL3* transcripts downstream of T-DNA insertions were absent in *cpl3–8* or *cpl3–9* mutants but present in *cpl3–7* mutant (Supplemental Figure S1, A and B). The *cpl3–7*, *cpl3–8*, and *cpl3–9* showed early flowering under long days and short days (Figure 1, C and D). Since these three mutants all exhibited similar flowering phenotypes, we chose *cpl3–8*, which contains a T-DNA insertion in the ninth exon, for further analysis.

To verify that the flowering defect of *cpl3–8* is caused by loss of *CPL3* function, we transformed *cpl3–8* with both *35S:CPL3-4HA* and a genomic construct (*gCPL3-4HA*) harboring a 6.5-kb *CPL3* genomic region including the 1.2-kb upstream sequence, the 4.7-kb coding sequence fused to the 4HA tag, and the 0.6-kb downstream sequence (Supplemental Figure S1A). Most of the T1 *cpl3–8 gCPL3-4HA* and *cpl3–8 35S:CPL3-4HA* transgenic plants showed comparable flowering time to wild-type (WT) plants (Figure 1E; Supplemental Figure S1, C and D), proving that the loss of *CPL3* results in the early flowering phenotype of *cpl3–8*. Together, these results suggest that *CPL3* plays an important role in repressing flowering in Arabidopsis.

To examine the expression pattern of *CPL3* during the floral transition, we generated a *pCPL3:β-glucuronidase* (*GUS*) reporter construct in which the same 1.2-kb *CPL3* upstream sequence included in *gCPL3-4HA* for the complementation test was fused to the *GUS* reporter gene (Supplemental

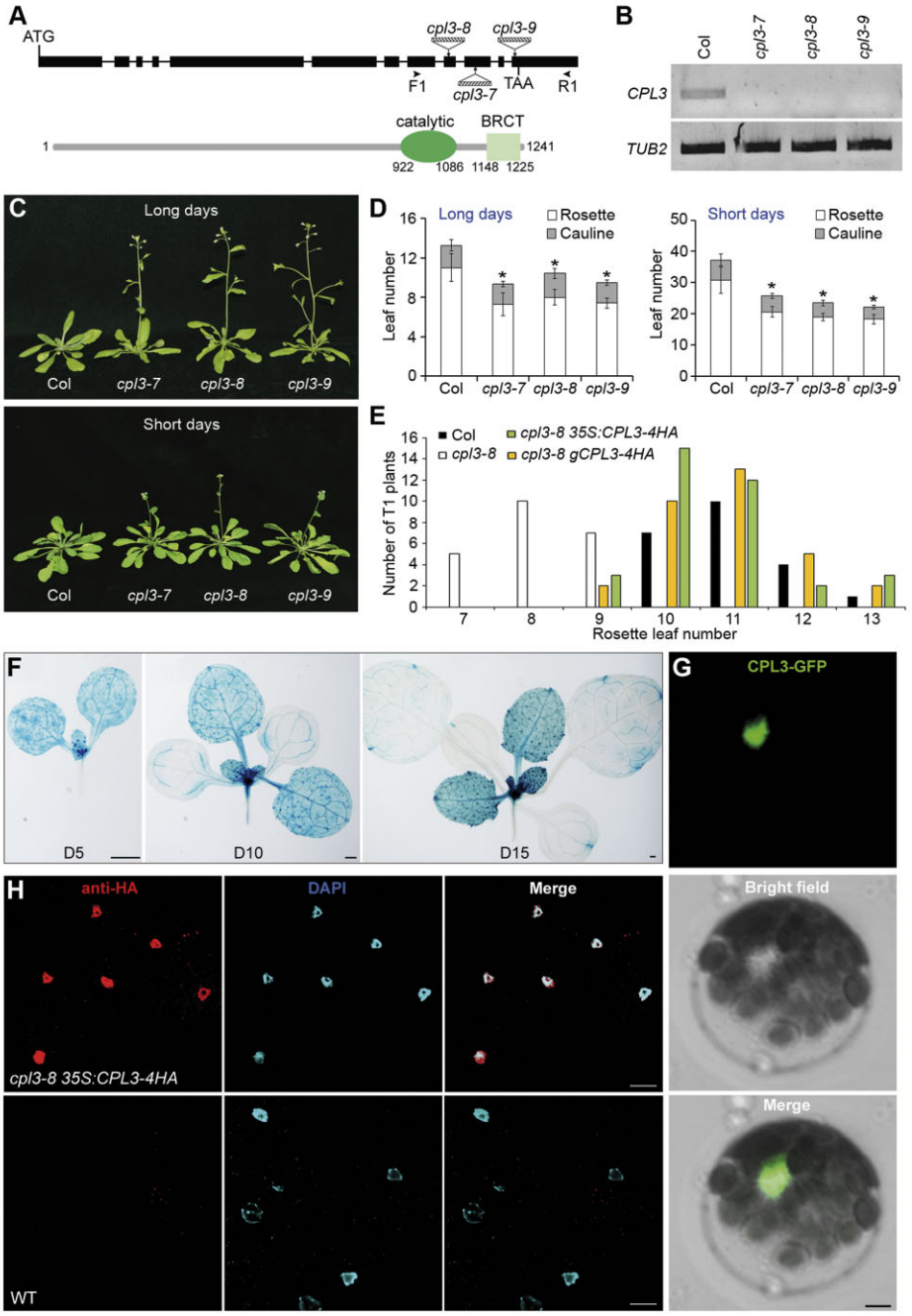

Figure 1 *CPL3* regulates flowering time in Arabidopsis. A, Schematic diagram shows the T-DNA insertion sites in *cpl3* mutants (upper part) and domain structure of CPL3 protein (lower part). Exons and introns in the coding region are indicated by black boxes and lines, respectively. *cpl3–7* (SALK_017644), *cpl3–8* (SALK_051322), and *cpl3–9* (SALK_019820) were obtained from the Arabidopsis Information Resource. Arrowheads indicate the positions of primers used for amplifying the *CPL3* fragment shown in Figure 1B. CPL3 contains a phosphatase catalytic domain and a BRCT domain. B, RT-PCR shows that *CPL3* expression is undetectable in *cpl3–7*, *cpl3–8*, and *cpl3–9* mutants using primers labeled in (A). *TUB2* was amplified as an internal control. C, *cpl3* exhibit early flowering under both long days (upper part) and short days (lower part). D, Flowering time of *cpl3* mutants under long days (right part) and short days (left part). Error bars, mean ± SD; n = 15. Asterisks denote significant differences for flowering time of *cpl3–7*, *cpl3–8*, and *cpl3–9* as compared with that of WT (Col) (two-tailed paired Student's t test, $P < 0.001$). E, Flowering time distribution of T1 transgenic plants of *cpl3–8 gCPL3-4HA* and *cpl3–8 35S:CPL3-4HA*. F, Representative GUS staining of *pCPL3:GUS* transgenic plants showing *CPL3* expression in a 5-day-old seedling (D5), a 10-day-old seedling (D10), a 15-day-old seedling (D15). Bars = 1 mm. G, Localization of CPL3-GFP in an Arabidopsis protoplast. *35S:CPL3-GFP* was transfected into Arabidopsis protoplasts and observed under a confocal microscope. Upper part, CPL3-GFP fluorescence; middle part, bright field; lower part, merge of CPL3-GFP and bright field. Bar = 10 μm. H, Immunolocalization of CPL3-4HA in protoplast cells isolated from *cpl3–8 35S:CPL3-4HA*. Protoplasts isolated from WT plants were used as negative controls. DAPI, fluorescence of 4′,6′-diamino-2-phenylindol; Merge, merge of anti-HA and DAPI images. Bars = 20 μm.

Figure S1A). We examined developing *pCPL3:GUS* seedlings before (Day 5), during (Day 10), and after (Day 15) the floral transition, which occurred 9–13 days after germination in our growth conditions. In these seedlings, strong GUS signals were detected in shoot apices, and vascular and mesophyll tissues of newly formed rosette leaves, and weaker signals were detected in vascular tissues of older leaves (Figure 1F), suggesting that *CPL3* is expressed in actively proliferating tissues during the floral transition. GUS signals were also found in mature rosette leaves in part of vascular tissues, cauline leaves, inflorescence meristems, flower buds, and siliques (Supplemental Figure S2, A–D). This staining pattern was consistent with the reverse transcription-quantitative polymerase chain reaction (PCR) results showing *CPL3* expression in all tissues tested with the highest expression in juvenile rosette leaves (Supplemental Figure S2E).

We also examined the subcellular localization of CPL3 in Arabidopsis protoplasts and found that CPL3-GFP localized specifically in the nucleus (Figure 1G). Further immunostaining of a functional *cpl3–8 35S:CPL3-4HA* line (Supplemental Figure S1C) confirmed the localization of CPL3-4HA protein in nucleus (Figure 1H; Supplemental Figure S1D).

To understand how *CPL3* influences flowering in response to flowering signals, we examined whether *CPL3* expression was regulated by environmental or endogenous flowering signals. *CPL3* expression was not greatly changed in various mutants of the autonomous and photoperiod pathways (Supplemental Figure S3, A and B), indicating that *CPL3* expression is not regulated by these pathways. Similarly, vernalization and gibberellic acid treatment did not affect *CPL3* expression (Supplemental Figure S3, C and D). These observations indicate that *CPL3* transcription may be not regulated by these flowering pathways. In addition, *cpl3–8* mutants responded normally to the changes in ambient temperature (Supplemental Figure S3E), implying that *CPL3* is also not involved in the thermosensory pathway.

CPL3 promotes *FLC* expression

To study the mechanism by which *CPL3* regulates the floral transition, we first identified the potential downstream targets of *CPL3* by comparing the expression levels of key flowering regulators in *cpl3* and WT (Col) seedlings. We examined the expression of two floral pathway integrators, *SOC1* and *FT*, and several other known flowering regulators, including *SHORT VEGETATIVE PHASE* (*SVP*), *FLC*, and its closely related *MADS AFFECTING FLOWERING 1–5* (*MAF1–5*). In line with the early flowering phenotype of *cpl3* mutants, both *FT* and *SOC1* were upregulated in *cpl3* mutants (Figure 2A). Notably, *FLC* expression was dramatically downregulated in all three *cpl3* mutants (Figure 2A). Further temporal expression analysis revealed that *FLC* expression was constantly and substantially downregulated in developing *cpl3–8* seedlings during the floral transition (Figure 2B), and *FT* and *SOC1* levels were consistently upregulated (Figure 2, C and D). The upregulation of *FT* and *SOC1* may be due to the dramatically decreased *FLC* expression in *cpl3–8* mutants, as FLC directly represses *FT* and *SOC1* expression (Helliwell et al., 2006). In contrast, the expression of *MAF1–5* genes, the FLC partner SVP (Li et al., 2008), and the *FLC* upstream regulators in the autonomous pathway were not greatly changed in *cpl3* mutants (Supplemental Figure S4, A–H). Moreover, in *cpl3–8 gCPL3-4HA* displaying comparable *CPL3* expression and flowering time to WT (Col) plants, *FLC* expression was restored (Figure 2, E and F; Supplemental Figure S1D). Since the Col ecotype contains a naturally occurring null allele of *fri*, these results suggest that CPL3 is required for establishing *FLC* basal expression in the absence of *FRI*.

We further studied the genetic interaction between *CPL3* and *FLC*. The *cpl3–8* and *flc-3* single and double mutants exhibited a similar early flowering phenotype under long days (Figure 2, G and H), indicating that *CPL3* and *FLC* could regulate flowering in the same genetic pathway. These results support the idea that CPL3 represses flowering mainly through activating *FLC* expression.

CPL3 is required for FRI-dependent activation of *FLC*

Given that CPL3 is necessary for *FLC* expression in Col, a rapid-cycling summer annual, we further explored whether CPL3 is also required for activating *FLC* in winter annuals. To this end, we crossed *cpl3–8* mutants with *FRI*-Col (Lee and Amasino, 1995), in which *FRI* elevates *FLC* expression to inhibit flowering (Johanson et al., 2000; Gazzani et al., 2003; Michaels et al., 2003). *cpl3–8* greatly suppressed the extremely late-flowering phenotype of *FRI* (Figure 2, I and J). Consistent with this suppression, *FLC* expression was significantly reduced in *FRI cpl3–8* as compared with *FRI* (Figure 2J). We further crossed the *FRI FLC:GUS* (Tao et al., 2017) with *cpl3–8*. FLC:GUS signals were reduced in *FRI cpl3–8* as compared with those in *FRI* (Figure 2K). These results suggest that CPL3 is also required for FRI-dependent activation of *FLC*. Taken together, our data show that CPL3 is indispensable for *FLC* expression in both winter annuals and rapid-cycling accessions of Arabidopsis.

Interaction of CPL3, FLX, and FLX4

As CPLs encode CTD phosphatase-like proteins that have been reported to dephosphorylate different types of proteins (Manavella et al., 2012; Della Monica et al., 2015), we reasoned that CPL3 could modulate *FLC* expression through dephosphorylating *FLC* upstream regulator(s). This prompted us to search for this regulator(s) based on two characteristics pertaining to CPL3-mediated regulation of *FLC*. First, CPL3 is rather specific in affecting *FLC* expression and its associated flowering effect, as *cpl3* mutants do not exhibit clear pleiotropic developmental defects, except alteration in flowering (Figure 1C). Second, CPL3 is required for both basal *FLC* expression in the rapid-cycling ecotype and FRI-dependent activation of *FLC* (Figure 2). These characteristics are shared with several components of the FRI-C, such as FLX, FLX4, FES1, and SUF4 (Schmitz et al., 2005; Kim et al., 2006; Kim and Michaels, 2006; Andersson et al., 2008;

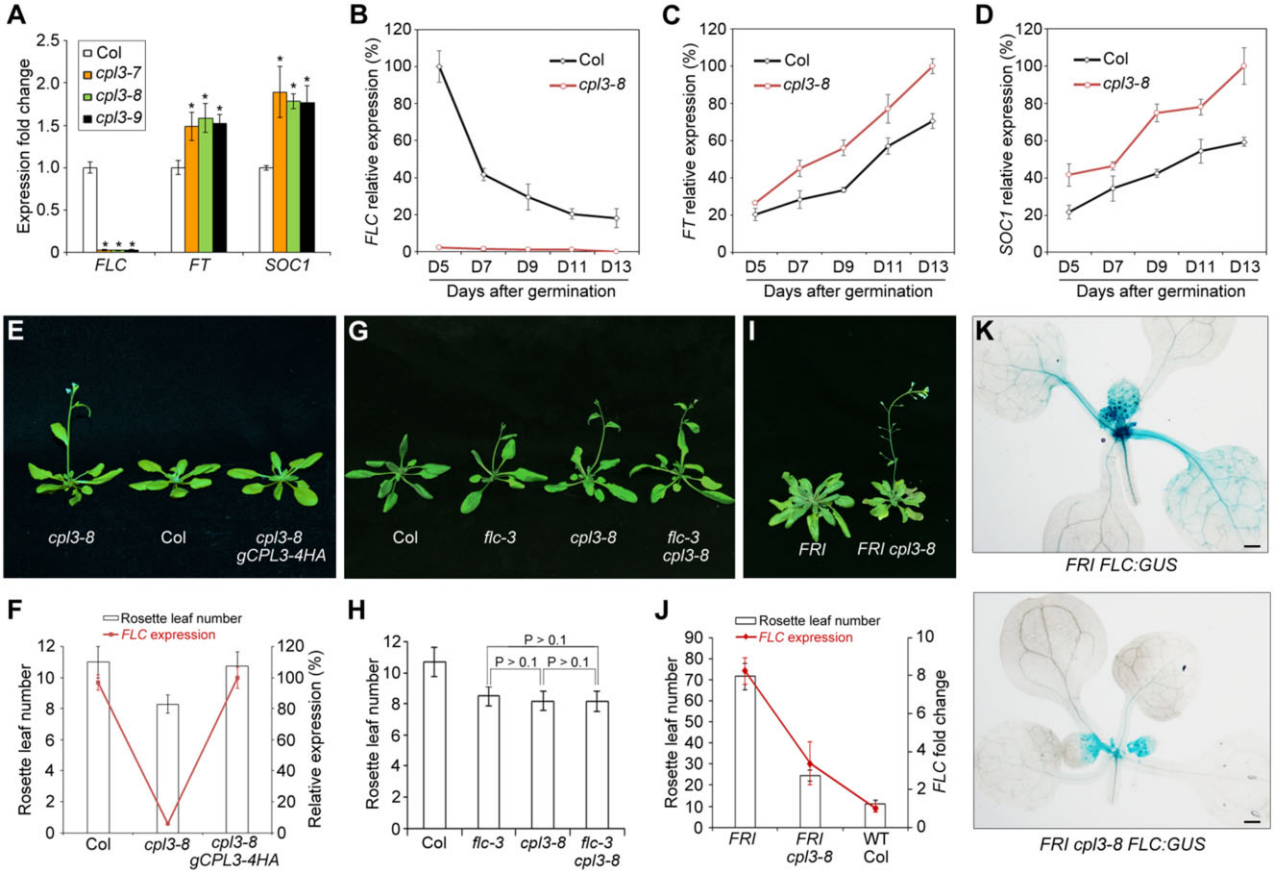

Figure 2 CPL3 regulates *FLC* expression. A, Expression analysis of *FLC*, *FT*, and *SOC1* in 9-day-old WT (Col) and various *cpl3* mutants. Error bars, mean ± SD; $n = 3$ biological replicates (independent pools of aerial parts of seedlings). Asterisks denote significant differences in expression levels of indicated genes in *cpl3–7*, *cpl3–8*, and *cpl3–9* as compared with those of WT (Col) (two-tailed paired Student's *t* test, $P < 0.05$). Approximately 15 seedlings were collected for each sample. B–D, Temporal expression of *FLC* (B), *FT* (C), and *SOC1* (D) in developing WT (Col) and *cpl3-8* seedlings under long days. The levels of gene expression normalized to *TUB2* expression are shown relative to the maximal expression level set at 100%. Error bars, mean ± SD; $n = 3$ biological replicates (independent pools of aerial parts of seedlings). Approximately 15 seedlings were collected for each sample. E, A representative line of *cpl3–8 gCPL3-4HA* shows comparable flowering time with WT (Col). F, Flowering time and *FLC* expression in WT (Col), *cpl3–8* and *cpl3–8 gCPL3-4HA* plants. Levels of *FLC* expression normalized to *TUB2* expression are shown relative to the maximal expression level set at 100%. Error bars, mean ± SD; $n = 3$ biological replicates (*FLC* expression; independent pools of aerial parts of seedlings); $n = 20$ (rosette leaf number). Approximately 15 seedlings were collected for each sample for gene expression analysis. G, Flowering phenotype of *flc-3 cpl3–8*. H, Flowering time of *flc-3 cpl3–8*. Error bars, mean ± SD; $n = 20$. There is no statistically significant difference in flowering time of *flc-3 cpl3–8*, *cpl3–8*, and *flc-3* (two-tailed paired Student's *t* test, $P > 0.1$). I, *cpl3* greatly suppresses the late-flowering phenotype of *FRI*. J, Comparison of flowering time and *FLC* expression in 9-day-old *FRI cpl3-8* and *FRI* plants under long days. Expression of *FLC* in WT (Col) was set as 1.0. Error bars, mean ± SD; $n = 3$ biological replicates (*FLC* expression; independent pools of aerial parts of seedlings); $n = 15$ (Rosette leaf number). Approximately 15 seedlings were collected for each sample for gene expression analysis. K, GUS staining of 11-day-old seedlings of *FRI FLC-GUS* (upper part) and *FRI cpl3-8 FLC-GUS* (lower part). Bars = 1 mm.

Choi et al., 2011; Ding et al., 2013; Lee and Amasino, 2013), while mRNA expression of these regulators remained unchanged in *cpl3–8* mutants (Supplemental Figure S5A).

Therefore, we first tested whether CPL3 interacts with any of these known *FLC*-specific regulators. Yeast two-hybrid (Y2H) assays revealed that CPL3 interacted with FLX (Figure 3A), which encodes a putative leucine zipper domain protein with transcriptional activation activity (Andersson et al., 2008; Choi et al., 2011). To determine which part of CPL3 is responsible for its interaction with FLX, we further performed Y2H assays using its N-terminus (CPL3-N) without any characterized domain and its C terminus (CPL3-C) containing the catalytic domain and the BRCT domain (Figure 3B), and found that the N-terminus is required for CPL3 interaction with FLX (Figure 3B). Bimolecular fluorescence complementation (BiFC) assays also revealed the direct interaction between CPL3 and FLX in the nuclei of living plant cells (Figure 3C). Furthermore, coimmunoprecipitation (CoIP) analysis confirmed the in vivo interaction of CPL3 and FLX in Arabidopsis seedlings expressing fully functional CPL3-4HA and FLX-3myc (Figure 3D; Supplemental Figure S6, A–E). Although the close linkage of *CPL3* (*At2g33540*) and *FLX* (*At2g30120*) on chromosome 2 prevented us from creating double mutants,

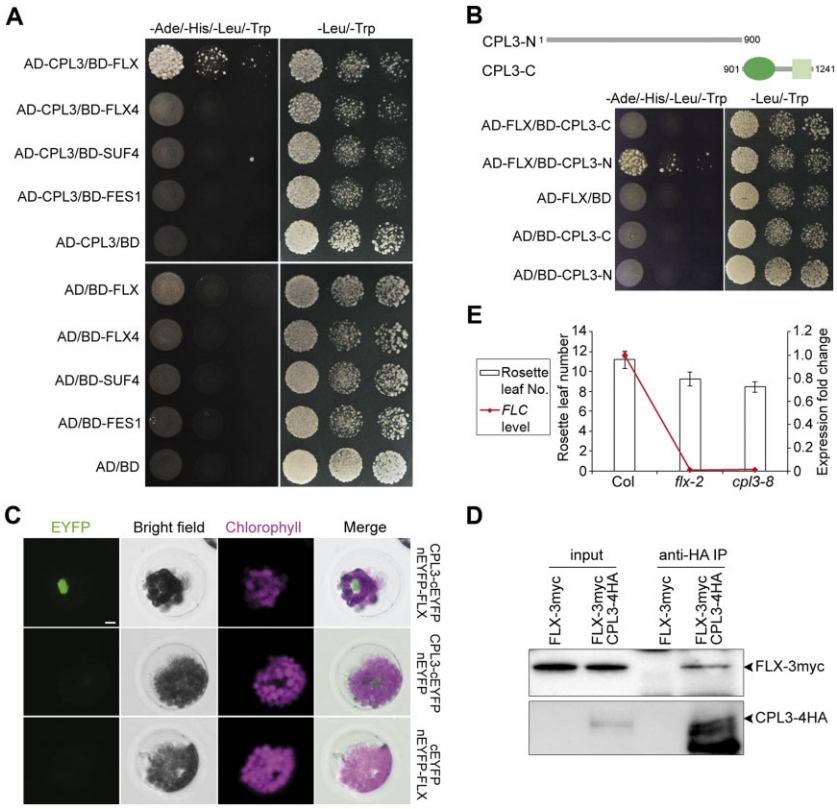

Figure 3 CPL3 Interacts with FLX. A, Y2H assays show the interaction between CPL3 and FLX. Serial dilutions (1:1, 1:5, 1:20) of transformed yeast cells were grown on SD−Ade/−His/−Leu/−Trp (left part) and SD−Leu/−Trp mediums (right part). B, Y2H assays show the interaction between FLX and CPL3-N. Schematic diagrams of CPL3 truncated proteins that were fused to BD are shown in the upper part. Serial dilutions (1:1, 1:5, and 1:20) of transformed yeast cells were grown on SD−Ade/−His/−Leu/−Trp (left part) and SD−Leu/−Trp (right part) mediums. C, BiFC analysis of the interaction between CPL3 and FLX. EYFP, fluorescence of enhanced yellow fluorescent protein; Merge, merge of EYFP, bright field, and chlorophyll. Bar = 10 μm. D, CoIP experiment shows the in vivo interaction between CPL3 and FLX. Nuclear proteins from F1 crossed seedlings of *cpl3–8 gCPL3-4HA* and *gFLX-3myc FRI flx-2* were extracted and incubated with anti-HA agarose. The immunoprecipitated proteins and protein extracts as input were detected by anti-myc (upper part) and anti-HA (lower part) antibodies. E, Flowering time and *FLC* expression in *cpl3–8* and *flx-2*. *FLC* expression in WT (Col) was set as 1.0. Error bars, mean ± SD; $n = 3$ biological replicates (*FLC* expression; independent pools of aerial parts of seedlings); $n = 15$ (Rosette leaf number). Approximately 15 seedlings were collected for each sample for gene expression analysis.

the comparable flowering time and *FLC* expression levels in *flx-2* and *cpl3–8* under long days (Figure 3E) support the idea that these two proteins interact to regulate *FLC* expression.

FLX, as an FRI-C complex component, directly interacts with FLX4 and FES1 within this complex (Supplemental Figure S5B; Choi et al., 2011; Ding et al., 2013). To test whether FLX acts to link CPL3 with other proteins in the FRI-C complex, including FLX4 or FES1, we performed yeast three-hybrid (Y3H) assays and revealed that CPL3 interacted with FLX4, but not FES1 in the presence of FLX (Figure 4A). The *flx4–2* and *cpl3–8* mutants exhibited comparable flowering times, which were associated with decreased *FLC* expression (Ding et al., 2013; Figure 4B). In agreement with their protein interactions, *CPL3*, *FLX*, and *FLX4* shared similar expression patterns in shoot apices, young leaves, and vasculatures of older leaves (Figure 4C) as well as other Arabidopsis tissues (Supplemental Figures S2, A–D, S7, and S8). These three proteins also colocalized in the nuclei of Arabidopsis protoplasts (Figure 4D).

CoIP assays in *Nicotiana benthamiana* further confirmed the protein interactions among CPL3, FLX, and FLX4 (Supplemental Figure S9A). Moreover, we generated *gFLX4-3FLAG FRI flx4-2* transgenic plants, in which *gFLX4-3FLAG* fully suppressed the early flowering of *FRI flx4-2* (Supplemental Figures S9, B and C), and further confirmed the interaction between CPL3 and FLX4 in Arabidopsis (Figure 4E). In addition, the *cpl3–8 flx4–2* mutants exhibited similar flowering times to *cpl3–8* (Figure 4B), supporting the idea that *CPL3* and *FLX4* function in the same genetic pathway. Overall, these results suggest that CPL3 is associated with FLX4 through their common protein partner FLX in the nuclei in Arabidopsis.

CPL3 dephosphorylates FLX4

Given that CPL3 forms a protein complex with FLX and FLX4 (Figures 3 and 4), we proceeded to examine whether CPL3 dephosphorylates FLX or FLX4 in flowering time control. Both FLX-3myc and FLX-GFP proteins were detected as single forms regardless of the presence of CPL3 in the

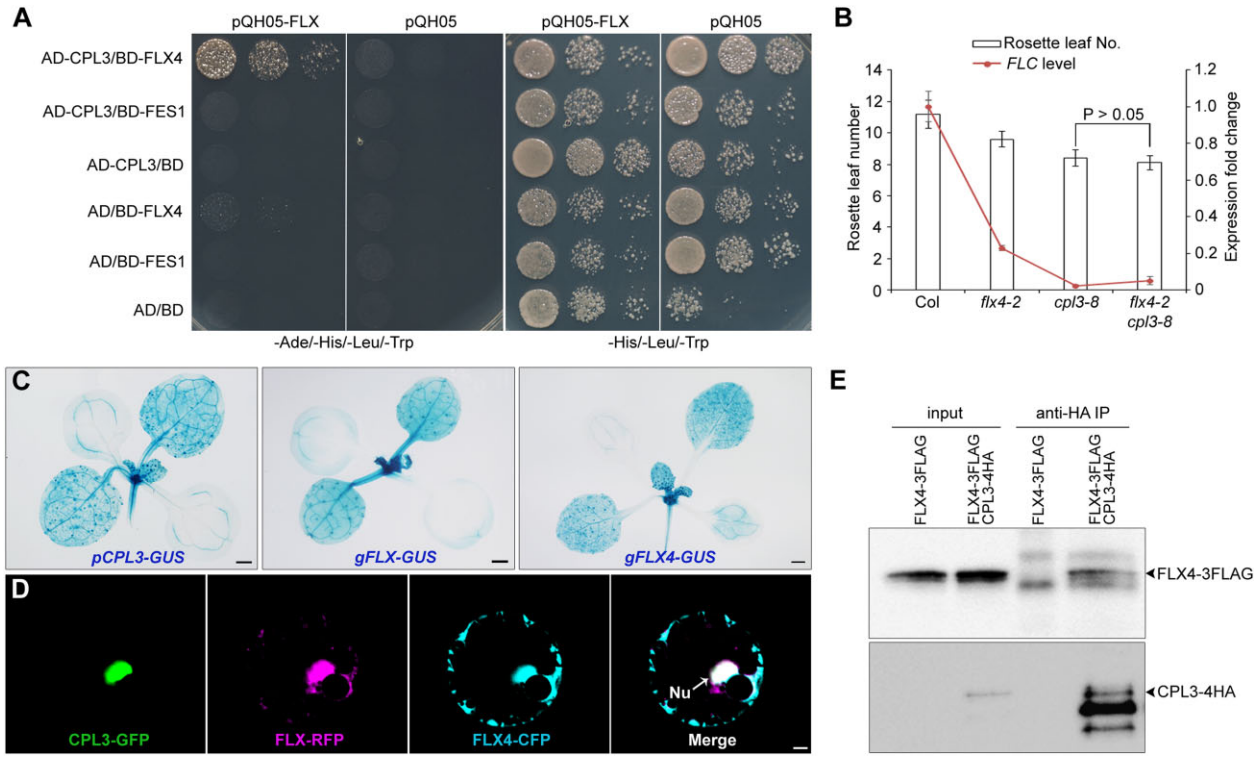

Figure 4 Interaction of CPL3, FLX, and FLX4. A, Y3H assays show the interaction between CPL3 and FLX4 in the presence of FLX. Either pQH05-FLX or pQH05 was co-transformed with various AD and BD plasmids. Serial dilutions (1:1, 1:5, 1:20) of transformed yeast cells were grown on SD−Ade/−His/−Leu/−Trp (left part) and SD−His/−Leu/−Trp (right part) mediums. B, Flowering time and *FLC* expression in *flx4−2 cpl3−8* double mutants. *FLC* expression in WT (Col) was set as 1.0. Error bars, mean ± SD; $n = 3$ biological replicates (*FLC* expression; independent pools of aerial parts of seedlings); $n = 20$ (Rosette leaf number). There is no statistically significant difference in flowering time of *flx4−2 cpl3−8*, and *cpl3−8* (two-tailed paired Student's *t* test, $P > 0.05$). Approximately 15 seedlings were collected for each sample for gene expression analysis. C, *CPL3*, *FLX*, and *FLX4* share similar tissue localization patterns in seedlings. GUS staining of 10-day-old *pCPL3:GUS*, *gFLX-GUS* and *gFLX4-GUS* seedlings are shown. Bars = 1 mm. D, Colocalization of CPL3-GFP, FLX-RFP, and FLX4-CFP in the nucleus of an Arabidopsis protoplast. *35S:CPL3-GFP*, *35S:FLX-RFP*, and *35S:FLX4-CFP* were co-transfected into Arabidopsis protoplasts. Merge, merge of CPL3-GFP, FLX-RFP, and FLX4-CFP images. Bar = 10 μm. E, CoIP experiment shows the in vivo interaction between CPL3 and FLX4. Nuclear proteins from F1 crossed seedlings of *cpl3−8 gCPL3-4HA*, and *gFLX4−3FLAG FRI flx4−2* were extracted and incubated with anti-HA agarose. The immunoprecipitated proteins and protein extracts as input were detected by anti-FLAG (upper part) and anti-HA (lower part) antibodies.

Phos-tag sodium dodecyl sulphate−polyacrylamide gel electrophoresis (SDS−PAGE) (Supplemental Figure S6, A–G), in which Phos-tag slows down the migration speed of phosphorylated proteins. Since this result suggests that FLX is not phosphorylated in vivo, FLX is unlikely the target for dephosphorylation by CPL3. CPL3 also did not affect the subcellular localization of FLX-GFP (Supplemental Figure S6H). In contrast, FLX4-4HA protein, when expressed in Arabidopsis protoplasts, existed in two phospho-isoforms in the presence of Phos-tag (Figure 5A). Treatment with the alkaline phosphatase CIAP confirmed that the more slowly migrating form of FLX4 is phosphorylated (Figure 5A).

To examine the phosphorylation of FLX4 in vivo, we generated *gFLX4-4HA* (Supplemental Figure S10A) and *35S:FLX4-4HA* tagging lines in *FRI flx4−2* (Figure 5, B–D). *flx4−2* completely suppresses the extremely delayed flowering phenotype of *FRI* (Ding et al., 2013; Lee and Amasino, 2013). Both *gFLX4-4HA* and *35S:FLX4-4HA* were able to rescue the rapid flowering of *FRI flx4−2*, suggesting that FLX4-4HA are fully functional. FLX4-4HA protein extracted from *gFLX4-4HA FRI flx4−2* and *35S:FLX4-4HA FRI flx4−2* existed in two phospho-isoforms in the presence of Phos-tag, and the more slowly migrating form was phosphorylated as confirmed by CIAP treatment (Figure 5E), suggesting that FLX4 is phosphorylated in vivo.

The phosphorylation status of FLX4-4HA was further substantiated by immunoblotting using the anti-Phospho-(Ser/Thr) antibody (Figure 5F). Notably, the level of phosphorylated FLX4-4HA protein was significantly increased in *cpl3−8* (Figure 5, G and H), suggesting that CPL3 functions in dephosphorylating FLX4. As rescue of rapid flowering of *FRI flx4−2* by *gFLX4-4HA* was largely compromised in the *cpl3−8* background (Figure 5D), CPL3-mediated dephosphorylation of FLX4 seems to be crucial for FLX4 function in regulating flowering time. Moreover, the phosphorylated FLX4-4HA protein levels were also increased in *flx-2* (Figure 5, G and

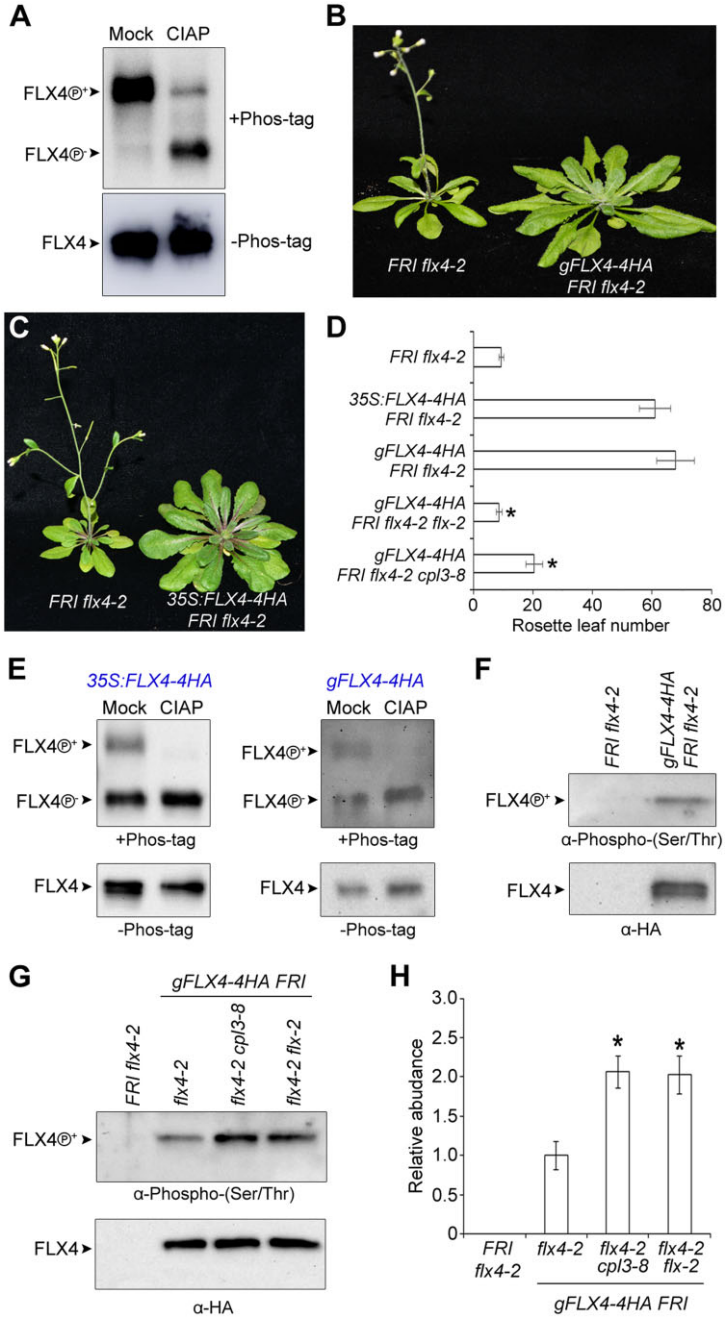

Figure 5 CPL3 mediates the dephosphorylation of FLX4. A, FLX4 is phosphorylated in Arabidopsis protoplasts. Protein extracts from Arabidopsis protoplasts transfected with *35S:FLX4-4HA* were immunoprecipitated using anti-HA agarose, followed by CIAP treatment for 3 h. Mock- or CIAP-treated proteins were resolved in polyacrylamide gels with (upper part) or without (lower part) Phos-tag. B and C, Representative transgenic lines of *gFLX4-4HA FRI flx4–2* (B) and *35S:FLX4-4HA FRI flx4–2* (C) display extremely late-flowering phenotype under long days. D, Comparison of flowering time of *FLX4* tagging lines in various genetic backgrounds grown under long days. Error bars, mean ± SD; $n = 15$. Asterisks denote significant differences in flowering time of indicated genotypes and *gFLX4-4HA FRI flx4–2* (two-tailed paired Student's *t* test, $P < 0.001$). E, FLX4 is phosphorylated in vivo. Mock or CIAP treatment of immunoprecipitated proteins from *35S:FLX4-4HA FRI flx4–2* (left part) and *gFLX4-4HA FRI flx4–2* (right part) were performed and the proteins were resolved in polyacrylamide gels with (upper part) or without (lower part) Phos-tag. F, Detection of FLX4 phosphorylation by anti-Phospho-(Ser/Thr) antibody. Immunoprecipitated proteins from *FRI flx4–2* and *gFLX4-4HA FRI flx4–2* were detected by anti-Phospho-(Ser/Thr) (upper part) and anti-HA (lower part) antibodies. G, The phosphorylated form of FLX4 was significantly increased in *cpl3–8* and *flx-2* mutants. Immunoprecipitated proteins from *FRI flx4–2*, *gFLX4-4HA FRI flx4–2*, *gFLX4-4HA FRI flx4–2 cpl3–8*, and *gFLX4-4HA FRI flx4–2 flx-2* were subjected to immunoblotting with anti-Phospho-(Ser/Thr) (upper part) and anti-HA (lower part) antibodies. H, Quantification of the phosphorylated FLX4 protein levels in (G). Asterisks indicate significant differences in phosphorylated FLX4 abundance between indicated genotypes and *gFLX4-4HA FRI flx4-2* (two-tailed paired Student's *t* test, $P < 0.05$). Densitometric analysis was performed on immunoblots from three biological replicates. The levels of phosphorylated FLX4 protein expression were normalized to total FLX4 protein levels. The phosphorylated FLX4 protein level in *gFLX4-4HA FRI flx4-2* was set as 1.0. Error bars, mean ± SD; $n = 3$.

H), supporting the role of FLX as a molecular link for CPL3-mediated dephosphorylation of FLX4.

CPL3-mediated FLX4 dephosphorylation is critical for regulating flowering time

To further determine the effect of CPL3-mediated FLX4 dephosphorylation in flowering time, we purified FLX4-4HA protein from *gFLX4-4HA FRI flx4–2* and determined its in vivo phosphorylation sites by mass spectrometry analysis. We found two phosphorylation sites, serine (S)171 and S226, located in the coiled-coil domain of FLX4 (Figure 6A; Supplemental Figure S11). Next, we generated phosphorylation-mimicking and dephosphorylation-mimicking forms of FLX4 to examine the effect of CPL3-mediated FLX4 dephosphorylation on flowering. We mutated the two identified phosphorylated sites individually to alanine (A) or aspartic acid (D) to generate the dephosphorylation-mimicking (gFLX4^{S171A}-4HA and gFLX4^{S226A}-4HA) or phosphorylation-mimicking (gFLX4^{S171D}-4HA and gFLX4^{S226D}-4HA) forms of FLX4, respectively. These constructs were transformed into *FRI flx4–2* plants. The WT FLX4-4HA, FLX4^{S171A}-4HA and FLX4^{S226A}-4HA, and FLX4^{S171D} proteins rather than FLX4^{S226D}-4HA protein rescued the rapid flowering phenotype of *FRI flx4–2* (Figure 6, B and C). The protein abundance of FLX4^{S226D}-4HA is comparable to that of FLX4-4HA or FLX4-4HA^{S226A}-4HA (Supplemental Figure S10B), suggesting that phosphorylation of FLX4 at the S226 residue inhibits its activity. Moreover, we introduced *gFLX4^{S226A}-4HA* and *gFLX4^{S226D}-4HA* into the *FRI cpl3–8* mutant background, and found that the dephosphorylation-mimicking FLX4 protein (FLX4^{S226A}) but not the phosphorylation-mimicking FLX4 protein (FLX4^{S226D}) partially suppressed the early flowering phenotype of *FRI cpl3–8* (Figure 6D), indicating that increased phosphorylation of FLX4 at S226 is at least partially responsible for the early flowering phenotype observed in *cpl3–8*.

As FLX4 is a component of the FRI-C activation complex that directly binds to the *FLC* locus to activate its expression (Choi et al., 2011), we further examined the binding of WT, dephosphorylation-mimicking, and phosphorylation-mimicking FLX4-4HA to the *FLC* locus by chromatin IP (ChIP) assays to understand how CPL3-mediated FLX4 dephosphorylation of S226 affects flowering. WT and dephosphorylation-mimicking FLX4^{S226A}-4HA proteins were associated with the *FLC* promoter region (Figure 6, E and F) and similarly bound by FRI-C (Choi et al., 2011). In contrast, phosphorylation-mimicking FLX4^{S226D}-4HA compromised FLX4 binding to the *FLC* locus (Figure 6F). Consistent with these effects, in *cpl3–8* mutants where FLX4 phosphorylation levels were increased, binding of FLX4-4HA to the *FLC* promoter region was significantly reduced (Figure 6G).

Since CPL3 and FLX4 are also required for establishing the basal *FLC* expression in the rapid-cycling Arabidopsis accession Col carrying a *fri* mutation (Figures 2 and 4B; Ding et al., 2013), we then tested whether CPL3-mediated dephosphorylation FLX4 also affects binding of FLX4 to *FLC* in rapid-cycling accessions. Again, binding of the phosphorylation-mimicking FLX4^{S226D}-4HA to the *FLC* locus was compromised (Figure 6H). Taken together, these results suggest that CPL3-mediated FLX4 dephosphorylation modulates the binding activity of FLX4 to the *FLC* locus, which is critical for regulating flowering time in both winter and summer Arabidopsis accessions.

Discussion

Precise regulation of the expression of *FLC*, the central floral repressor, engages many chromatin modifiers and transcription factors for flowering under optimal conditions to ensure reproductive success. Here we demonstrated that the plant CTD phosphatase CPL3 acts as an essential regulator required for both FRI-dependent *FLC* activation in the establishment of winter-annual habit and for FRI-independent *FLC* basal expression in the summer annuals. Through the molecular scaffold FLX, CPL3 interacts with and dephosphorylates FLX4 to facilitate the binding of dephosphorylated FLX4 to the *FLC* locus for activating *FLC* expression (Figure 7). Thus, dephosphorylation of FLX4 by CPL3 serves as a key molecular switch that secures the transcription of *FLC* mRNAs to prevent premature flowering under unfavorable conditions.

Our findings establish CPL3 as a flowering time regulator in modulating *FLC* expression through affecting the phosphorylation status of an *FLC* activator FLX4 mediated by FLX. Several pieces of evidence demonstrate that CPL3, FLX, and FLX4 act in the same pathway to regulate *FLC* expression. First, in the rapid-cycling accessions, *FLC* expression is dramatically decreased in *cpl3* mutants, while *flc*, *cpl3*, or their double mutant exhibits a similar early-flowering phenotype (Figure 2), suggesting that *FLC* is the major target of CPL3. This is consistent with the roles of FLX and FLX4 (Michaels et al., 2004; Schmitz et al., 2005; Kim et al., 2006; Kim and Michaels, 2006; Andersson et al., 2008; Choi et al., 2011; Ding et al., 2013; Lee and Amasino, 2013). Second, mutations in *CPL3*, *FLX* and *FLX4* result in similarly early-flowering phenotypes in the Col background and reduced *FLC* levels, and the *flx4 cpl3* double mutant does not further enhance the flowering phenotype of *cpl3*, supporting the idea that the three genes function in the same genetic pathway to regulate *FLC* expression. Third, in winter annuals, *cpl3*, *flx*, or *flx4* greatly suppresses the late-flowering of *FRI* (Figure 2; Michaels et al., 2004; Schmitz et al., 2005; Kim et al., 2006; Kim and Michaels, 2006; Andersson et al., 2008; Choi et al., 2011; Ding et al., 2013; Lee and Amasino, 2013), further corroborating that they function in the same genetic pathway in establishing the winter annual habit. Moreover, CPL3 forms a protein complex with FLX and FLX4, in which CPL3 dephosphorylates FLX4. FLX protein is not phosphorylated, excluding the possibility that FLX is a target of dephosphorylation by CPL3. Mutations in *CPL3* increase the phosphorylated protein levels of FLX4 (Figure 5G), suggesting that CPL3 specifically dephosphorylates FLX4. Phosphorylated protein levels of FLX4 are also significantly increased when *FLX* is lost (Figure 5G), corroborating the

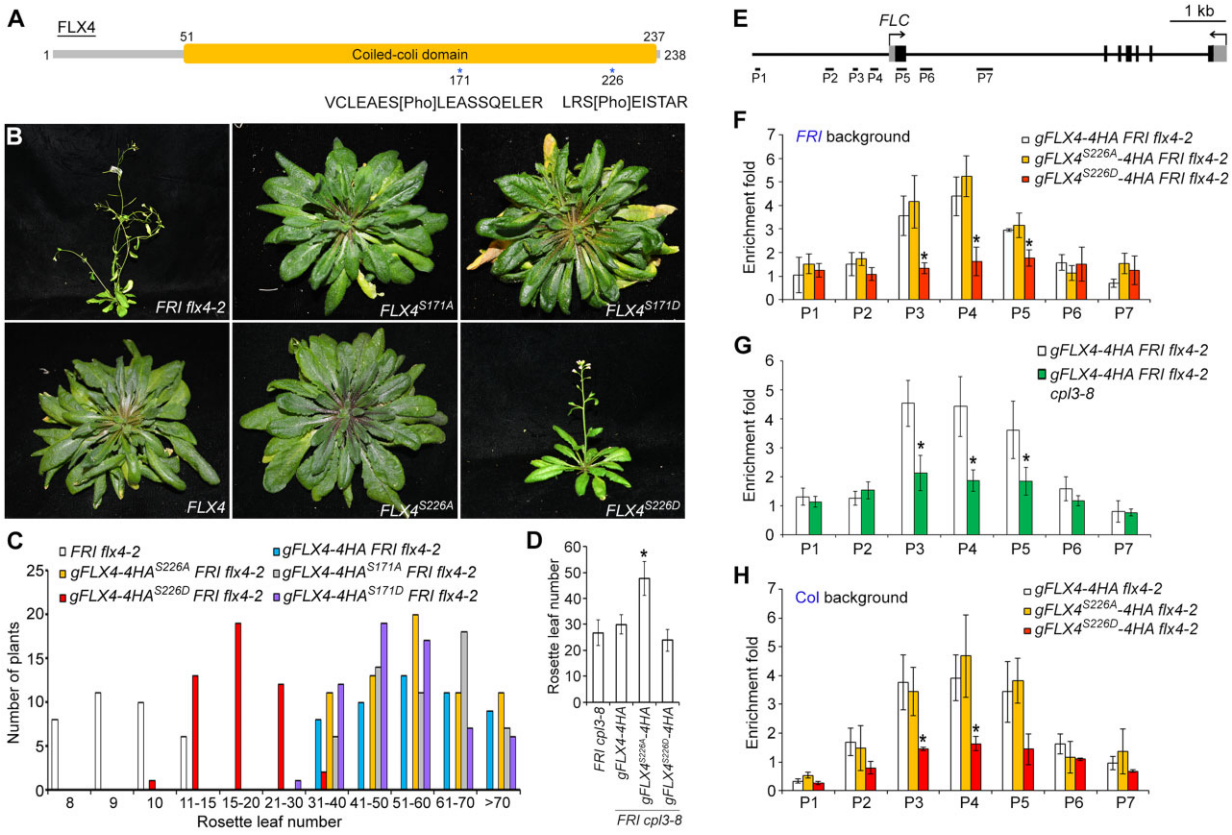

Figure 6 CPL3-mediated dephosphorylation of FLX4 enables its repressive role in flowering and binding to the *FLC* locus. A, Schematic diagram showing the protein domain structure of FLX4 and the identified phosphorylated peptides and sites of FLX4 in the coiled-coil domain. The domain structure of FLX4 was predicated by SMART (http://smart.embl-heidelberg.de/) (Letunic and Bork, 2018). Blue asterisks indicate the positions of potentially phosphorylated Ser residues. B, Effects of mutated FLX4 proteins on flowering time under long days. Representative *FRI flx4-2*, *gFLX4-4HA FRI flx4–2*, *gFLX4*^{S171A}*-4HA FRI flx4–2*, *gFLX4*^{S171D}*-4HA FRI flx4–*, *gFLX4*^{S226A}*-4HA FRI flx4–2*, and *gFLX4*^{S226D}*-4HA FRI flx4–2* plants were shown. C, Flowering time distribution of various transgenic lines under long days. *gFLX4-4HA*, *gFLX4*^{S171A}*-4HA*, *gFLX4*^{S171D}*-4HA*, *gFLX4*^{S226A}*-4HA*, and *gFLX4*^{S226D}*-4HA* were transformed into *FRI flx4–2* mutants, and the flowering time of T1 transgenic lines were recorded. D, Flowering time of *FRI cpl3-8* in the presence of *gFLX-4HA*, *gFLX4-4HA*^{S226A} and *gFLX4-4HA*^{S226D}. Error bars, mean ± SD; $n = 15$. Asterisks denote significant differences in flowering time of *gFLX4-4HA*^{S226A} *FRI cpl3-8*, and *FRI cpl3–8* (two-tailed paired Student's *t* test, $P < 0.001$). E, Schematic diagram showing the genomic region of *FLC* and positions of primers used in ChIP assays. Exons in coding regions and untranslated regions (UTRs) are shown by black and gray boxes, respectively, while introns and promoter regions are shown by black lines. Bend arrows denote the transcription start site and transcription termination site. Seven primers located in the promoter region and within the first intron of *FLC* were used in ChIP assays shown in (F–H). F, ChIP analysis of the binding of FLX4 native protein, its phosphorylation-mimicking and dephosphorylation-mimicking forms to the *FLC* locus in tagging lines generated under the *FRI* background. Error bars, mean ± SD; $n = 4$ biological replicates (independent pools of aerial parts of seedlings). Asterisks denote significant differences in ChIP enrichment folds between *gFLX4-4HA*^{S226D} *FRI flx4–2*, and *gFLX4-4HA FRI flx4–2* (two-tailed paired Student's *t* test, $P < 0.05$). G, ChIP analysis of the binding of FLX4 to the *FLC* locus in *FRI flx4-2* and *FRI flx4-2 cpl3-8*. Error bars, mean ± SD; $n = 4$ biological replicates (independent pools of aerial parts of seedlings). Asterisks denote significant differences in ChIP enrichment folds between *gFLX4-4HA FRI flx4–2 cpl3–8* and *gFLX4-4HA FRI flx4–2* (two-tailed paired Student's *t* test, $P < 0.05$). H, ChIP analysis of the binding of FLX4 native protein, its phosphorylation-mimicking and dephosphorylation-mimicking forms to the *FLC* locus in tagging lines under the Col background. Error bars, mean ± SD; $n = 4$ biological replicates (independent pools of aerial parts of seedlings). Asterisks denote significant differences in ChIP enrichment folds between *gFLX4-4HA*^{S226D} *flx4–2* and *gFLX4-4HA flx4–2* (two-tailed paired Student's *t* test, $P < 0.05$).

role of FLX as a scaffold in mediating the dephosphorylation of FLX4 by CPL3. Thus, we have uncovered a CPL3-FLX-FLX4 module that determines *FLC* expression for the precise regulation of flowering time.

CPL3-mediated dephosphorylation of FLX4 serves as a molecular switch that prevents premature flowering. Phosphorylation of FLX4 at residue of serine 226 weakens its association with the *FLC* promoter (Figure 6, F–H) in both winter annuals and the rapid-cycling Col accession. Previous studies have suggested that SUF4 recruits FRI-C to the *FLC* proximal promoter (Kim et al., 2006), and that SUF4 is also important for *FLC* expression in the summer annuals (Ding et al., 2013). Thus, it is possible that SUF4 mediates binding of dephosphorylated FLX4 to the *FLC* promoter region regardless of the presence or absence of *FRI*. Since both dephosphorylated and phosphorylated FLX4 proteins exist in vivo in functional FLX4 tagging lines (Figure 5E), CPL3 may function in concert with other unknown kinase(s) to

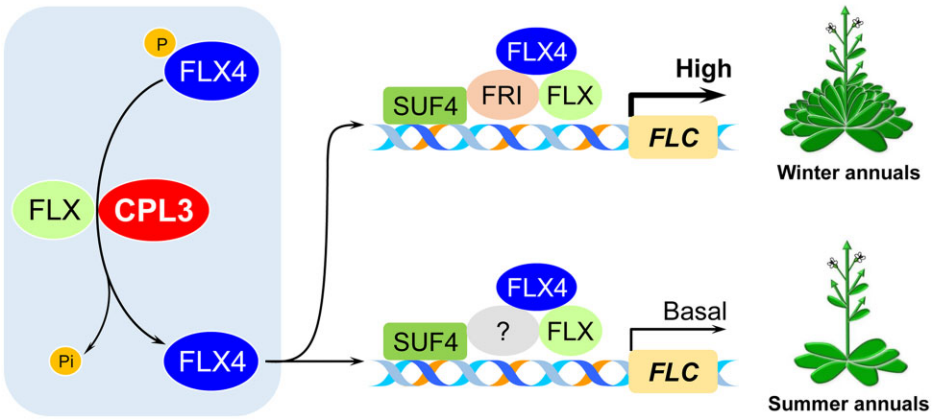

Figure 7 A Molecular switch for *FLC* activation in Arabidopsis. The plant CTD phosphatase CPL3 interacts with and dephosphorylates FLX4 mediated by their scaffold protein FLX. This molecular switch is indispensable for *FLC* activation in winter annuals, and for *FLC* basal expression in summer annuals. In the presence of CPL3, CPL3 dephosphorylates FLX4, which facilitates the binding of dephosphorylated FLX4 to the *FLC* locus in both winter and summer annuals and the incorporation of FLX4 into the FRI complex in the winter annuals, thus establishing *FLC* levels required for flowering at the appropriate time. In the absence of CPL3, the phosphorylated form of FLX4 is increased, resulting in reduced *FLC* expression and precocious flowering.

balance relative levels between dephosphorylated and phosphorylated states of FLX4 to determine *FLC* levels required for the appropriate control of flowering time.

CPL3 interacts with FLX and FLX4, both of which are essential components of the FRI-C, suggesting that CPL3 may be involved in the FRI supercomplex. Similar to other individual components involved in FRI-dependent *FLC* activation in the FRI supercomplex (Choi et al., 2011; Li et al., 2018), loss of *CPL3* compromises *FLC* activation and causes premature flowering, indicating that each component is indispensable for the function of the supercomplex as a whole in controlling flowering. FRI-mediated *FLC* upregulation requires the RNA Pol II-associated PAF1c, and the nuclear cap-binding complex that may enhance RNA Pol II activity (He et al., 2004; Oh et al., 2004; Geraldo et al., 2009; Crevillen and Dean, 2011; Li et al., 2016). Interestingly, CPL3 has been shown to mediate the dephosphorylation of Pol II in vitro and in vivo to regulate plant immune responses (Koiwa et al., 2004; Li et al., 2014). In the yeast *Saccharomyces cerevisiae*, dephosphorylation of the Pol II CTD by the CPL3 ortholog Fcp1 regulates the association of capping enzymes with Pol II during gene transcription (Schroeder et al., 2000). Thus, we envisage that CPL3 may possess additional functions besides dephosphorylating FLX4 to activate *FLC*, which may include dephosphorylation of Pol II. Moreover, phosphorylation of Pol II CTD by the cyclin-dependent kinase CDKC;2 is involved in *FLC* antisense transcript-mediated repression of *FLC* (Wang et al., 2014). It would be interesting to explore whether the Pol II dephosphorylation by CPL proteins is relevant to this process.

Plant CPLs have different impacts on flowering (Figure 1; Koiwa et al., 2002; Ueda et al., 2008) and the CPL3-FLX-FLX4 functional mode may exist for other CPLs, allowing them to engage other flowering regulators and have different effects on flowering. Besides flowering, CPLs also function in various biological processes. For example, CPL3 also regulates the immune response as well as RNA metabolism and silencing (Li et al., 2014, 2019). Thus, further uncovering the interacting proteins of CPLs will be critical for understanding their functional modes and specificities in regulating various developmental processes or stress responsiveness. As CTD phosphatase family proteins are conserved among eukaryotes (Ghosh et al., 2008), the functional mode of CPL3 revealed in this study sheds important light on the roles of CTD phosphatases in mediating key developmental processes through dephosphorylating important regulatory proteins.

Materials and methods

Plant materials and growth conditions

Seeds of Arabidopsis (*A. thaliana*) were put on soil (BVB soil mixture: sand = 4:1) or Murashige and Skoog (MS) agar plates and stratified at 4°C in darkness for 3 days before they are moved to growth or tissue culture rooms. Arabidopsis plants were grown on soil or MS medium under long days (16-h light/8-h dark) or short days (8-h light/16-h dark), illuminated by white light-emitting diodes (135–150 μmol m^{-2} s^{-1}, at 23 ± 2°C or 16 ± 1°C. The mutants of *cpl3–7* (SALK_017644), *cpl3-8* (SALK_051322), *cpl3–9* (SALK_019820), and *flk-2* (SALK_001523) were obtained from the Arabidopsis Information Resource. The mutants of *flx-2* and *FRI flx4–2* were kindly provided by Prof. Scott Michaels (Indiana University) and the seed of *FLC:GUS* in *FRI flc-3* mutant background was given by Prof. Yuehui He (Peking University). The *cpl3–7*, *cpl3–8*, *cpl3–9*, *flc-3*, *ft-10*, *co-9*, *gi-1*, *fd-2*, *fve-4*, *flk-2*, *fld-3*, and *flx-2* mutants are in the Col background, and *fpa-1* mutants are in the *Ler* background. *Agrobacterium tumefaciens*-mediated transformation of Arabidopsis Col plants or various mutants was carried out by the floral dipping method (Clough and Bent, 1998).

Plasmid construction

To construct *gCPL3-4HA*, the 5.9-kb genomic sequence of *CPL3* containing the 1.2-kb upstream sequence, the 4.7-kb coding sequence plus introns were amplified with gCPL3-F and CPL3-R(HindIII) and cloned into pENTR/D-TOPO (Invitrogen, Waltham, MA, USA) to generate *gCPL3*. Based on this construct, *4HA* sequence was cloned in frame with *gCPL3*, and subsequently the 0.6-kb downstream sequence of *CPL3* was introduced using a modified QuikChange site-directed mutagenesis method (Geiser et al., 2001) to generate *gCPL3-4HA*. To construct *35S:CPL3-4HA* or *35S:CPL3-GFP*, the coding sequence of *CPL3* was amplified with CPL3-F(HindIII) and CPL3-R(HindIII) and cloned into a modified pENTR vector with *35S* promoter and *4HA* sequence (pENTR-35S-4HA) or pGreen 0229 35S-GFP (Shen et al., 2016) to obtain an in-frame fusion of *35S:CPL3-4HA* or *35S:CPL3-GFP*, respectively. To construct *pCPL3:GUS*, the 1.2-kb upstream sequence of *CPL3* was amplified with pCPL3-F(PstI) and pCPL3-R(XmaI), and cloned into a modified pENTR vector with the *GUS* gene (pENTR-GUS).

To generate *gFLX-3myc*, *gFLX-GFP*, or *gFLX-GUS*, the genomic sequence of *FLX* amplified with gFLX-F(PstI) and gFLX-R(XmaI) were cloned into modified pENTR vectors with *3myc* (pENTR-3myc), *GFP* (pENTR-GFP), or *GUS* (pENTR-GUS), respectively. To construct *35S:FLX-9myc*, the coding sequence of *FLX* was amplified with FLX-F(PstI) and FLX-R(XmaI), and cloned into the modified pENTR-35S:9myc vector. Similarly, FLX coding sequence was cloned into pGreen 0229-35S-RFP to generate *35S:FLX-RFP*.

To generate *gFLX4-4HA* and *gFLX4-GUS*, the genomic sequence of *FLX4* was amplified with gFLX4-F(XmaI) and FLX4-R(XmaI) and cloned into pGreen-4HA (Shen et al., 2016) and pENTR-GUS, respectively. To generate *gFLX4-3FLAG*, the genomic sequence of FLX4 was amplified and cloned into a modified pENTR-3FLAG vector. The coding sequence of *FLX4* amplified with FLX4-F(PstI) and FLX4-R(XmaI) was cloned into a modified pENTR-35S-4HA vector to generate *35S:FLX4-4HA*. Based on the constructs of *gFLX4-4HA*, *gFLX4*^{S171A}*-4HA*, *gFLX4*^{S171D}*-4HA*, *gFLX4*^{S226A}*-4HA*, and *gFLX4*^{S226D}*-4HA* were generated by overlapping PCR. The coding sequence of *FLX4* amplified with FLX4-F(HindIII) and FLX4-R(PstI) were cloned into the modified pENTR vectors, pENTR-35S-3FLAG and pENTR-35S-CFP to generate *35S:FLX4-3FLAG* and *35S:FLX4-CFP*, respectively.

The primers used for plasmid construction are listed in Supplemental Table S1.

Expression analysis

Total RNA was extracted using the RNeasy Plus Mini Kit (Qiagen, Hilden, Germany) and reverse transcribed with the M-MLV Reverse Transcriptase (Promega, Madison, WI, USA) according to the manufacturers' instructions. Quantitative real-time PCR was performed on three biological replicates with SYBR Green PCR Master Mix (Applied Biosystems, Waltham, MA, USA) using 7900HT Fast Real-Time PCR systems (Applied Biosystems). The expression of *TUBULIN 2* (*TUB2*) was included as an internal control. The difference between the cycle threshold (C_t) of target genes and the Ct of control primers ($\Delta C_t = C_{ttarget\ gene} - C_{tcontrol}$) was used to calculate the normalized expression of target genes. The list of primers used for gene expression analysis is shown in Supplemental Table S1.

GUS staining

GUS staining of *pCPL3:GUS*, *gFLX-GUS*, *gFLX4-GUS*, *FRI FLC:GUS*, and *FRI cpl3–8 FLC:GUS* transgenic plants was performed as previously described with minor modifications (Shen et al., 2014). Seedlings were fixed in ice-cold 90% acetone for 20 min and washed 3 times with rinse solution [50 mM Na_2HPO_4, 50 mM NaH_2PO_4, 0.5 mM $K_3Fe(CN)_6$, 0.5 mM $K_4Fe(CN)_6$]. The seedlings or plant tissues were then infiltrated with staining solution (rinse solution with 2 mM X-Gluc) under vacuum followed by incubation at 37°C for several hours. The stained plants were cleared of chlorophyll in an ethanol series and observed under a light microscope in the clearing solution (7.5 g of gum arabic, 100 g of chloral hydrate, 5 mL of glycerol and 30 mL of H_2O).

Immunolocalization

Immunolocalization of CPL3-4HA in Arabidopsis root and protoplasts was performed as previously described (Lee et al., 2013). Protoplasts were isolated from leaves of 12-day-old seedlings of WT or *cpl3–8 35S:CPL3-4HA* grown on soil, whereas roots were collected from WT or *cpl3–8 35S:CPL3-4HA* grown on MS medium. Immunolocalization was performed with anti-HA antibody (sc-7392, Santa Cruz Dallas, TX, USA) and CF555 goat anti-mouse IgG antibody (Biotium San Francisco, CA, USA) served as primary and secondary antibodies, respectively. The slides were examined under a confocal microscope.

Y2H and Y3H assays

The coding sequences of *CPL3*, *CPL3*-N, *CPL3*-C, *FLX*, *FLX4*, *SUF4*, *FES1*, and *FRI* were amplified and cloned into pGBKT7 (BD) or pGADT7 (AD) vectors (Clontech, Glasgow, UK). The primers used for cloning were listed in Supplemental Table S1. The various AD and BD vectors were co-transformed into Y2HGold yeast cells using the Yeastmaker Yeast Transformation System 2 according to the manufacturer's instructions (Clontech). The transformed yeast cells were selected on SD–Ade/–His/–Leu/–Trp medium.

For Y3H assay, the *FLX* coding sequence was amplified and cloned into pQH05 (Hou et al., 2014) with a *HIS3* selection marker. Yeast Y2HGold cells co-transformed with various AD and BD vectors with *pQH05* or *pQH05-FLX* were selected on SD-Ade/-His/-Leu/-Trp medium.

Protein expression in *N. benthamiana* cells and Arabidopsis mesophyll protoplasts

Agrobacterium cultures with various expression vectors were harvested and diluted in infiltration buffer (10 mM MES, pH

5.6, 10 mM $MgCl_2$ with freshly added 100 μM acetosyringone) to optical density (OD_{600nm}) at 0.6. The *Agrobacteria* were infiltrated into the abaxial surface of 3-week-old *N. benthamiana* leaves with syringes.

Mesophyll Arabidopsis protoplasts were isolated and transfected as previously reported (Wu et al., 2009). To examine the protein localization of CPL3 and colocalization of CPL3/FLX/FLX4, *35S:CPL3-GFP* plasmid or the mixture of *35S:CPL3-GFP/35S:FLX-RFP/35S:FLX4-CFP* plasmids were transfected into protoplasts and incubated under low light conditions for 16–20 h before being examined under a confocal microscope.

CoIP

Nine-day-old seedlings from F1 crossed seedlings of *cpl3–8 gCPL3-4HA* and *gFLX-3myc FRI flx-2*, *cpl3–8 35S:CPL3-4HA* and *gFLX-3myc FRI flx-2*, *cpl3–8 gCPL3-4HA* and *gFLX4-3FLAG FRI flx4–2*, or *N. benthamiana* leaves coinfiltrated with *35S:FLX-9myc/35S:CPL3-4HA/35S:FLX4-3FLAG* were collected. Nuclear proteins extracted from these materials were incubated 4 h with anti-HA agarose conjugate (Sigma St Louis, MO, USA) at 4°C. The immunoprecipitated proteins and protein extracts as input were resolved by SDS–PAGE and detected by anti-HA (Santa Cruz, Cat# sc-7392 HRP, 1:1,000 dilution), anti-myc (Santa Cruz, Cat# sc-40, 1:1,000 dilution) or anti-FLAG M2 (Sigma, Cat#F3165, 1:1,000 dilution) antibodies.

BiFC analysis

Full-length coding regions of *CPL3* and *FLX* were cloned into the primary pSAT1 vectors (Citovsky et al., 2006). The resulting cassettes including the constitutive promoters and fusion proteins were cloned into pHY105 (Liu et al., 2007). The plasmids were co-transfected into Arabidopsis protoplasts and the transfected protoplasts were examined under a confocal microscope.

Alkaline phosphatase treatment

Alkaline phosphatase treatment of FLX4 protein was carried out as previously described (Wang et al., 2010). FLX4-4HA proteins extracted from protoplasts transfected with *35S:FLX4-4HA*, or transgenic plants of *35S:FLX4-4HA FRI flx4–2* and *gFLX-4HA FRI flx4–2* were immunoprecipitated with anti-HA agarose conjugate (Sigma). After IP, the agarose beads were washed twice with alkaline buffer (50 mM Tris–HCl pH 8.8, 1 mM $MgCl_2$) and then once with CIAP buffer supplemented with protease inhibitors. Subsequently, the beads were resuspended in CIAP buffer and incubated with or without CIAP at 37°C for 3 h. After CIAP or mock treatment, SDS loading buffer was added for SDS–PAGE or Phos-tag SDS–PAGE followed by immunoblot analysis with anti-HA antibody (Sigma).

Phos-tag SDS–PAGE

Phos-tag SDS–PAGE was performed as previously described (Chen et al., 2020). SDS–PAGE gels containing 50 μM Phos-tag (Wako Pure Chemical Industries, Richmond, VA, USA) and 100 μM $MnCl_2$ were used. After electrophoresis, the protein gel with Phos-tag was washed 3 times with transfer buffer (25 mM Tris, 192 mM glycine, 20% methanol) supplemented with 10 mM EDTA, and then washed with transfer buffer followed by blotting and detection with appropriate antibodies, such as anti-HA antibody (Santa Cruz, Cat# sc-7392 HRP, 1:1,000 dilution), anti-myc antibody (Santa Cruz, Cat# sc-40, 1:1,000 dilution), and anti-GFP antibody (Santa Cruz, Cat# sc-9996, 1:1,000 dilution).

Mass spectrometry analysis

Nuclear protein was extracted from 9-day-old seedlings of *gFLX4-4HA FRI flx4–2* with nuclear isolated buffer (20 mM KCl, 25% glycerol, 20 mM Tris pH 7.0, 30 mM β- mercaptoethanol, 2.5 mM $MgCl_2$, 0.7% Triton X-100, 2 mM EDTA pH 8.0, 250 mM sucrose) with freshly added 1× protease inhibitor cocktail (Roche, Basel, Switzerland) and 1× phosphatase inhibitor cocktail 3 (Sigma-Aldrich, St Louis, MO, USA), and resuspended in IP buffer (50 mM HEPES pH 7.5, 150 mM KCl, 10 μM $ZnSO_4$, 0.05% SDS, 5 mM $MgCl_2$, 1% Triton X-100, 1× protease inhibitor cocktail, 1× phosphatase inhibitor cocktail 3). The nuclear extract was incubated with anti-HA agarose (Sigma-Aldrich) for 4 h at 4°C. After washing, the immunoprecipitated protein was eluted and analyzed by mass spectrometry with a TripleTOF 5600 System (AB Sciex, Protein and Proteomics Centre in National University of Singapore). The mass spectrometry analysis of *gFLX4-4HA FRI flx4–2* was repeated 2 times and the mass spectra of the identified phosphorylated peptides were shown in Supplemental Figure S11.

ChIP assay

ChIP assay was carried out in various genetic background as previously described with minor modifications (Shen et al., 2011). Nine-day-old seedlings were collected, ground in liquid nitrogen and postfixed with 1% formaldehyde for 10 min. The chromatin was extracted and sonicated to generate DNA fragments of around 500 bp. The solubilized chromatin was incubated with anti-HA agarose conjugate (Sigma) for 4 h at 4°C. ChIP experiments were repeated with three biological replicates. The genomic fragment of *TUB2* was included as the internal control. Enrichment fold of each fragment was determined by quantitative real-time PCR as previously described (Li et al., 2008). Briefly, fold enrichment of each fragment was calculated first by normalizing the level of a target DNA fragment against that of the internal control fragment, and then by normalizing the value for immunoprecipitated samples against that for input. The primer pairs used for ChIP assays are shown in Supplemental Table S1.

Statistical analysis

The detailed statistical analyses of the experiments are available in the figure legends, including the statistical test used, exact value of n and what n represents. Statistical tests were conducted using Microsoft Excel. Quantification of

immunoblot signals was performed by tracing out the individual band using ImageJ (https://imagej.nih.gov/ij/).

Accession numbers

Sequence data from this article can be found in the GenBank/EMBL data libraries under the following accession numbers: *CPL3* (At2g33540), *FES1* (At2g33835), *FLC* (At5g10140), *FLX* (At2g30120), *FLX4* (At5g61920), *FRI* (At4g00650), *FT* (At1g65480), and *SOC1* (At2g45660).

Supplemental data

The following materials are available in the online version of this article.

Supplemental Figure S1. Generation of *CPL3* tagging lines and *CPL3* expression.

Supplemental Figure S2. Expression patterns of *CPL3*.

Supplemental Figure S3. *CPL3* expression in response to various flowering signals.

Supplemental Figure S4. Expression of various flowering time genes in *cpl3* mutants.

Supplemental Figure S5. FLX interacts with FLX4 and FES1.

Supplemental Figure S6. FLX is not phosphorylated in vivo.

Supplemental Figure S7. Expression pattern of *FLX* in Arabidopsis.

Supplemental Figure S8. Expression pattern of *FLX4* in Arabidopsis.

Supplemental Figure S9. Interaction of CPL3, FLX, and FLX4.

Supplemental Figure S10. Phosphorylation of FLX4 does not affect its protein abundance.

Supplemental Figure S11. Mass spectra of the phosphorylated peptides identified from the nuclear protein extracts from 9-day-old seedlings of *gFLX4-4HA FRI flx4–2*.

Supplemental Table S1. List of primers used in this study.

Supplemental Table S2. Summary of statistical analysis (two-tailed paired Student's t test).

Acknowledgments

We thank the Arabidopsis Biological Resource Centre, Prof. Scott Michaels, and Prof. Yuehui He for providing seeds. We thank Prof Hao Yu and his lab for discussion and comments on this manuscript, and the Protein and Proteomics Centre in the Department of Biological Sciences, National University of Singapore for mass spectrometry service.

Funding

This work was supported by the National Research Foundation Competitive Research Program (NRF-CRP22-2019-0001), the Agency for Science, Technology, and Research (A*STAR) under its Industry Alignment Fund - Pre Positioning (A19D9a0096), and the intramural research support from Temasek Life Sciences Laboratory.

Conflict of interest statement. None declared.

References

Andersson CR, Helliwell CA, Bagnall DJ, Hughes TP, Finnegan EJ, Peacock WJ, Dennis ES (2008) The FLX gene of Arabidopsis is required for FRI-dependent activation of FLC expression. Plant Cell Physiol **49:** 191–200

Andres F, Coupland G (2012) The genetic basis of flowering responses to seasonal cues. Nat Rev Genet **13:** 627–639

Ausin I, Alonso-Blanco C, Jarillo JA, Ruiz-Garcia L, Martinez-Zapater JM (2004) Regulation of flowering time by FVE, a retinoblastoma-associated protein. Nat Genet **36:** 162–166

Bao S, Hua C, Shen L, Yu H (2020) New insights into gibberellin signaling in regulating flowering in Arabidopsis. J Integr Plant Biol **62:** 118–131

Chen Y, Song S, Gan Y, Jiang L, Yu H, Shen L (2020) SHAGGY-like kinase 12 regulates flowering through mediating CONSTANS stability in Arabidopsis. Sci Adv **6:** eaaw0413

Cho EJ, Kobor MS, Kim M, Greenblatt J, Buratowski S (2001) Opposing effects of Ctk1 kinase and Fcp1 phosphatase at Ser 2 of the RNA polymerase II C-terminal domain. Genes Dev **15:** 3319–3329

Cho H, Kim TK, Mancebo H, Lane WS, Flores O, Reinberg D (1999) A protein phosphatase functions to recycle RNA polymerase II. Genes Dev **13:** 1540–1552

Choi K, Kim J, Hwang HJ, Kim S, Park C, Kim SY, Lee I (2011) The FRIGIDA complex activates transcription of FLC, a strong flowering repressor in Arabidopsis, by recruiting chromatin modification factors. Plant Cell **23:** 289–303

Citovsky V, Lee LY, Vyas S, Glick E, Chen, M.H., Vainstein, A., Gafni, Y., Gelvin, S.B., Tzfira, T. (2006) Subcellular localization of interacting proteins by bimolecular fluorescence complementation in planta. J Mol Biol **362:** 1120–1131

Clarke JH, Dean C (1994) Mapping FRI, a locus controlling flowering time and vernalization response in *Arabidopsis thaliana*. Mol Gen Genet **242:** 81–89

Clough SJ, Bent AF (1998) Floral dip: a simplified method for Agrobacterium-mediated transformation of *Arabidopsis thaliana*. Plant J **16:** 735–743

Crevillen P, Dean C (2011) Regulation of the floral repressor gene FLC: the complexity of transcription in a chromatin context. Curr Opin Plant Biol **14:** 38–44

Della Monica R, Visconti R, Cervone N, Serpico AF, Grieco D (2015) Fcp1 phosphatase controls Greatwall kinase to promote PP2A-B55 activation and mitotic progression. Elife **4**: e10399

Ding L, Kim SY, Michaels SD (2013) FLOWERING LOCUS C EXPRESSOR family proteins regulate FLOWERING LOCUS C expression in both winter-annual and rapid-cycling Arabidopsis. Plant Physiol **163:** 243–252

Gazzani S, Gendall AR, Lister C, Dean C (2003) Analysis of the molecular basis of flowering time variation in Arabidopsis accessions. Plant Physiol **132:** 1107–1114

Geiser M, Cebe R, Drewello D, Schmitz R (2001) Integration of PCR fragments at any specific site within cloning vectors without the use of restriction enzymes and DNA ligase. Biotechniques **31:** 88–92

Geraldo N, Baurle I, Kidou S, Hu X, Dean C (2009) FRIGIDA delays flowering in Arabidopsis via a cotranscriptional mechanism involving direct interaction with the nuclear cap-binding complex. Plant Physiol **150:** 1611–1618

Ghosh A, Shuman S, Lima CD (2008) The structure of Fcp1, an essential RNA polymerase II CTD phosphatase. Mol Cell **32:** 478–490

He Y, Michaels SD, Amasino RM (2003) Regulation of flowering time by histone acetylation in Arabidopsis. Science **302:** 1751–1754

He Y, Doyle MR, Amasino RM (2004) PAF1-complex-mediated histone methylation of FLOWERING LOCUS C chromatin is required for the vernalization-responsive, winter-annual habit in Arabidopsis. Genes Dev **18:** 2774–2784

Helliwell CA, Wood CC, Robertson M, James Peacock W, Dennis ES (2006) The Arabidopsis FLC protein interacts directly in vivo with SOC1 and FT chromatin and is part of a high-molecular-weight protein complex. Plant J **46:** 183–192

Hepworth SR, Valverde F, Ravenscroft D, Mouradov A, Coupland G (2002) Antagonistic regulation of flowering-time gene SOC1 by CONSTANS and FLC via separate promoter motifs. EMBO J **21:** 4327–4337

Hou X, Zhou J, Liu C, Liu L, Shen L, Yu H (2014) Nuclear factor Y-mediated H3K27me3 demethylation of the SOC1 locus orchestrates flowering responses of Arabidopsis. Nat Commun **5:** 4601

Jiang D, Gu X, He Y (2009) Establishment of the winter-annual growth habit via FRIGIDA-mediated histone methylation at FLOWERING LOCUS C in Arabidopsis. Plant Cell **21:** 1733–1746

Jin YM, Jung J, Jeon H, Won SY, Feng Y, Kang JS, Lee SY, Cheong JJ, Koiwa H, Kim M (2011) AtCPL5, a novel Ser-2-specific RNA polymerase II C-terminal domain phosphatase, positively regulates ABA and drought responses in Arabidopsis. New Phytol **190:** 57–74

Johanson U, West J, Lister C, Michaels S, Amasino R, Dean C (2000) Molecular analysis of FRIGIDA, a major determinant of natural variation in Arabidopsis flowering time. Science **290:** 344–347

Kim DH, Sung S (2012) Environmentally coordinated epigenetic silencing of FLC by protein and long noncoding RNA components. Curr Opin Plant Biol **15:** 51–56

Kim S, Choi K, Park C, Hwang HJ, Lee I (2006) SUPPRESSOR OF FRIGIDA4, encoding a C2H2-Type zinc finger protein, represses flowering by transcriptional activation of Arabidopsis FLOWERING LOCUS C. Plant Cell **18:** 2985–2998

Kim SY, Michaels SD (2006) SUPPRESSOR OF FRI 4 encodes a nuclear-localized protein that is required for delayed flowering in winter-annual Arabidopsis. Development **133:** 4699–4707

Koiwa H, Hausmann S, Bang WY, Ueda A, Kondo N, Hiraguri A, Fukuhara T, Bahk JD, Yun DJ, Bressan RA, et al. (2004) Arabidopsis C-terminal domain phosphatase-like 1 and 2 are essential Ser-5-specific C-terminal domain phosphatases. Proc Natl Acad Sci USA **101:** 14539–14544

Koiwa H, Barb AW, Xiong L, Li F, McCully MG, Lee BH, Sokolchik I, Zhu J, Gong Z, Reddy M, et al. (2002) C-terminal domain phosphatase-like family members (AtCPLs) differentially regulate *Arabidopsis thaliana* abiotic stress signaling, growth, and development. Proc Natl Acad Sci USA **99:** 10893–10898

Koornneef M, Blankestijn-de VH, Hanhart C, Soppe W, Peeters T (1994) The phenotype of some late-flowering mutants is enhanced by a locus on chromosome 5 that is not effective in the Landsberg erecta wild-type. Plant J **6:** 9

Lee I, Amasino RM (1995) Effect of vernalization, photoperiod, and light quality on the flowering phenotype of Arabidopsis plants containing the FRIGIDA gene. Plant Physiol **108:** 157–162

Lee I, Michaels S, Masshardt A, Amasino R (1994a) The late-flowering phenotype of FRIGIDA and mutations in LUMINIDEPENDENS is suppressed in the Landsberg erecta strain of Arabidopsis. Plant J **6:** 7

Lee I, Aukerman MJ, Gore SL, Lohman KN, Michaels SD, Weaver LM, John MC, Feldmann KA, Amasino RM (1994b) Isolation of LUMINIDEPENDENS: a gene involved in the control of flowering time in Arabidopsis. Plant Cell **6:** 75 –83

Lee J, Amasino RM (2013) Two FLX family members are non-redundantly required to establish the vernalization requirement in Arabidopsis. Nat Commun **4:** 2186

Lee MH, Lee Y, Hwang I (2013) In vivo localization in Arabidopsis protoplasts and root tissue. Methods Mol Biol **1043:** 113–120

Letunic I, Bork P (2018) 20 years of the SMART protein domain annotation resource. Nucleic Acids Res **46:** D493–D496

Li D, Liu C, Shen L, Wu Y, Chen H, Robertson M, Helliwell CA, Ito T, Meyerowitz E, Yu H (2008) A repressor complex governs the integration of flowering signals in Arabidopsis. Dev Cell **15:** 110–120

Li F, Cheng C, Cui F, de Oliveira MV, Yu X, Meng X, Intorne AC, Babilonia K, Li M, Li B, et al. (2014) Modulation of RNA polymerase II phosphorylation downstream of pathogen perception orchestrates plant immunity. Cell Host Microbe **16:** 748–758

Li T, Natran A, Chen Y, Vercruysse J, Wang K, Gonzalez N, Dubois M, Inze D (2019) A genetics screen highlights emerging roles for CPL3, RST1 and URT1 in RNA metabolism and silencing. Nat Plants **5:** 539–550

Li Z, Jiang D, He Y (2018) FRIGIDA establishes a local chromosomal environment for FLOWERING LOCUS C mRNA production. Nat Plants **4:** 836–846

Li Z, Jiang D, Fu X, Luo X, Liu R, He Y (2016) Coupling of histone methylation and RNA processing by the nuclear mRNA cap-binding complex. Nat Plants **2:** 16015

Liu C, Zhou J, Bracha-Drori K, Yalovsky S, Ito T, Yu H (2007) Specification of Arabidopsis floral meristem identity by repression of flowering time genes. Development **134:** 1901–1910

Macknight R, Bancroft I, Page T, Lister C, Schmidt R, Love K, Westphal L, Murphy G, Sherson S, Cobbett C, et al. (1997) FCA, a gene controlling flowering time in Arabidopsis, encodes a protein containing RNA-binding domains. Cell **89:** 737–745

Manavella PA, Hagmann J, Ott F, Laubinger S, Franz M, Macek B, Weigel D (2012) Fast-forward genetics identifies plant CPL phosphatases as regulators of miRNA processing factor HYL1. Cell **151:** 859–870

Michaels SD, Amasino RM (1999) FLOWERING LOCUS C encodes a novel MADS domain protein that acts as a repressor of flowering. Plant Cell **11:** 949–956

Michaels SD, Amasino RM (2001) Loss of FLOWERING LOCUS C activity eliminates the late-flowering phenotype of FRIGIDA and autonomous pathway mutations but not responsiveness to vernalization. Plant Cell **13:** 935–941

Michaels SD, Bezerra IC, Amasino RM (2004) FRIGIDA-related genes are required for the winter-annual habit in Arabidopsis. Proc Natl Acad Sci USA **101:** 3281–3285

Michaels SD, He Y, Scortecci KC, Amasino RM (2003) Attenuation of FLOWERING LOCUS C activity as a mechanism for the evolution of summer-annual flowering behavior in Arabidopsis. Proc Natl Acad Sci USA **100:** 10102–10107

Mockler TC, Yu X, Shalitin D, Parikh D, Michael TP, Liou J, Huang J, Smith Z, Alonso JM, Ecker JR, et al. (2004) Regulation of flowering time in Arabidopsis by K homology domain proteins. Proc Natl Acad Sci USA **101:** 12759–12764

Oh S, Zhang H, Ludwig P, van Nocker S (2004) A mechanism related to the yeast transcriptional regulator Paf1c is required for expression of the Arabidopsis FLC/MAF MADS box gene family. Plant Cell **16:** 2940–2953

Park S, Oh S, Ek-Ramos J, van Nocker S (2010) PLANT HOMOLOGOUS TO PARAFIBROMIN is a component of the PAF1 complex and assists in regulating expression of genes within H3K27ME3-enriched chromatin. Plant Physiol **153:** 821–831

Pose D, Yant L, Schmid M (2012) The end of innocence: flowering networks explode in complexity. Curr Opin Plant Biol **15:** 45–50

Schmitz RJ, Hong L, Michaels S, Amasino RM (2005) FRIGIDA-ESSENTIAL 1 interacts genetically with FRIGIDA and FRIGIDA-LIKE 1 to promote the winter-annual habit of *Arabidopsis thaliana*. Development **132:** 5471–5478

Schomburg FM, Patton DA, Meinke DW, Amasino RM (2001) FPA, a gene involved in floral induction in Arabidopsis, encodes a protein containing RNA-recognition motifs. Plant Cell **13:** 1427–1436

Schroeder SC, Schwer B, Shuman S, Bentley D (2000) Dynamic association of capping enzymes with transcribing RNA polymerase II. Genes Dev **14:** 2435–2440

Searle I, He Y, Turck F, Vincent C, Fornara F, Krober S, Amasino RA, Coupland G (2006) The transcription factor FLC confers a flowering response to vernalization by repressing meristem competence and systemic signaling in Arabidopsis. Genes Dev **20:** 898–912

Sheldon CC, Rouse DT, Finnegan EJ, Peacock WJ, Dennis ES (2000) The molecular basis of vernalization: the central role of FLOWERING LOCUS C (FLC). Proc Natl Acad Sci USA **97**: 3753–3758

Shen L, Kang YG, Liu L, Yu H (2011) The J-domain protein J3 mediates the integration of flowering signals in Arabidopsis. Plant Cell **23:** 499–514

Shen L, Thong Z, Gong X, Shen Q, Gan Y, Yu H (2014) The putative PRC1 RING-finger protein AtRING1A regulates flowering through repressing MADS AFFECTING FLOWERING genes in Arabidopsis. Development **141:** 1303–1312

Shen L, Liang Z, Gu X, Chen Y, Teo ZW, Hou X, Cai WM, Dedon PC, Liu L, Yu H (2016) N(6)-methyladenosine RNA modification regulates shoot stem cell fate in Arabidopsis. Dev Cell **38:** 186–200

Simpson GG, Dijkwel PP, Quesada V, Henderson I, Dean C (2003) FY is an RNA 3′ end-processing factor that interacts with FCA to control the Arabidopsis floral transition. Cell **113:** 777–787

Tao Z, Shen L, Gu X, Wang Y, Yu H, He Y (2017) Embryonic epigenetic reprogramming by a pioneer transcription factor in plants. Nature **551:** 124–128

Ueda A, Li P, Feng Y, Vikram M, Kim S, Kang CH, Kang JS, Bahk JD, Lee SY, Fukuhara T, et al. (2008) The *Arabidopsis thaliana* carboxyl-terminal domain phosphatase-like 2 regulates plant growth, stress and auxin responses. Plant Mol Biol **67:** 683–697

Wang Y, Liu C, Yang D, Yu H, Liou YC (2010) Pin1At encoding a peptidyl-prolyl cis/trans isomerase regulates flowering time in Arabidopsis. Mol Cell **37:** 112–122

Wang ZW, Wu Z, Raitskin O, Sun Q, Dean C (2014) Antisense-mediated FLC transcriptional repression requires the P-TEFb transcription elongation factor. Proc Natl Acad Sci USA **111:** 7468–7473

Whittaker C, Dean C (2017) The FLC locus: a platform for discoveries in epigenetics and adaptation. Annu Rev Cell Dev Biol **33:** 555–575

Wu FH, Shen SC, Lee LY, Lee SH, Chan MT, Lin CS (2009) Tape-Arabidopsis Sandwich - a simpler Arabidopsis protoplast isolation method. Plant Methods **5:** 16

Xu L, Menard R, Berr A, Fuchs J, Cognat V, Meyer D, Shen WH (2009) The E2 ubiquitin-conjugating enzymes, AtUBC1 and AtUBC2, play redundant roles and are involved in activation of FLC expression and repression of flowering in *Arabidopsis thaliana*. Plant J **57:** 279–288

Yu X, Michaels SD (2010) The Arabidopsis Paf1c complex component CDC73 participates in the modification of FLOWERING LOCUS C chromatin. Plant Physiol **153:** 1074–1084

Zhang H, van Nocker S (2002) The VERNALIZATION INDEPENDENCE 4 gene encodes a novel regulator of FLOWERING LOCUS C. Plant J **31:** 663–673